

Use of lithium-ion batteries in electric vehicles

B. Kennedy^{*}, D. Patterson, S. Camilleri

Northern Territory Centre for Energy Research, Northern Territory University, Darwin, NT 0909, Australia

Received 22 December 1999; received in revised form 1 February 2000; accepted 16 February 2000

Abstract

An account is given of the lithium-ion (Li-ion) battery pack used in the Northern Territory University's solar car, *Fuji Xerox Desert Rose*, which competed in the 1999 World Solar Challenge (WSC). The reasons for the choice of Li-ion batteries over silver–zinc batteries are outlined, and the construction techniques used, the management of the batteries, and the battery protection boards are described. Data from both pre-race trialling and race telemetry, and an analysis of both the coulombic and the energy efficiencies of the battery are presented. It is concluded that Li-ion batteries show a real advantage over other commercially available batteries for traction applications of this kind. © 2000 Elsevier Science S.A. All rights reserved.

Keywords: Lithium-ion battery; Electric vehicle; Rechargeable battery

1. Introduction

Lithium-ion (Li-ion) batteries are an attractive proposition for use in high-performance electric vehicles. In comparison with other rechargeable batteries, Li-ion provides very high specific energy and a large number of charge–discharge cycles. The cost is also reasonable. Thus, Li-ion batteries are the preferred choice over other technologies such as silver–zinc and nickel–metal-hydride. Presently, however, Li-ion batteries are only commercially available in small sizes. Accordingly, large numbers of cells have to be assembled in series/parallel configurations to achieve the desired battery sizes. This, combined with safety issues, presents the challenge of making highly efficient, highly reliable, battery packs for use in electric vehicles.

2. Background on World Solar Challenge

The World Solar Challenge (WSC) is the premiere event for solar-powered vehicles (so-called, ‘solar cars’). Starting from Darwin in Northern Australia, it crosses the continent and finishes in Adelaide, a distance of 3000 km.

The WSC has been run every 3 years since 1987. The winners have been: General Motors, USA (1987); the Engineering College of Biel, Switzerland (1990); Honda, Japan (1993, 1996); the Aurora Vehicle Association, Australia (1999). The Northern Territory University is one of only four teams to compete in all five of the WSC events held to date, and the only team to complete successfully all races. In 1999, the *Fuji Xerox Desert Rose* (Fig. 1) finished fourth overall and won its class, ‘Silicon Solar Cells, Exotic Batteries’, at an average speed of 71.00 km/h, just 68 min behind the winner after 5 days of racing.

3. WSC rules and battery regulations

The rules for building a solar car are simple [1] and can be summarized as follows.

- The box rule: the car must fit in a box which is 6 m long, 2 m wide, and 1.6 m high. The solar cells must have a projected horizontal area of no more than 8 m².
- The clock rule: cars may race only between 0800 and 1700 h; stationary charging of the batteries from the sun is allowed before and after these times, respectively.

^{*} Corresponding author.

E-mail address: byron.kennedy@ntu.edu.au (B. Kennedy).

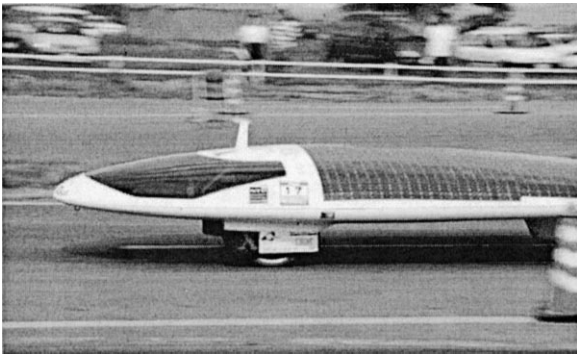


Fig. 1. *Fuji Xerox Desert Rose* solar car.

Other rules also govern the exact dimensions of the solar array, the procedure at media stops, and general safety criteria for the vehicles. Of particular interest are the regulations for battery size. The cells or battery modules must be rechargeable by the vehicles in which they are fitted. The total energy must be less than a nominal 5 kW h (20-h rate). This is determined on the basis of weight, namely, not more than 40 kg for silver–zinc (on the basis that the specific energy of this system is typically 125 W h/kg, so that 40 kg equates to 5 kW h), 40 kg for ‘advanced’ battery systems (e.g., lithium-ion), 75 kg for nickel–zinc, 71 kg for nickel–metal-hydride, 100 kg for nickel–cadmium and nickel–iron, and 125 kg for lead–acid. The limit applies only to the weight of the individual cells or batteries, that is, the weight of peripheral equipment (connectors, battery box, etc.) is not counted.

4. Solar car strategy

In order to build a fast solar car, it is essential to minimize the aerodynamic drag coefficient, the frontal area

of the vehicle, the tyre rolling resistance and the weight of the vehicle. In parallel, the energy efficiencies of the vehicle components, i.e., solar array, motor and battery, must all be maximized.

A common strategy for a solar car is to race throughout the day at a constant speed and to end the day with a precalculated amount of energy stored in the batteries. Typically, the battery capacity will be at 40% state-of-charge (SoC) at the end of the first day, and at zero SoC at the end of the fifth day. As mentioned above, after racing has finished, time is available in the afternoon and next morning to recharge the batteries from the sun. The battery profile for the *Fuji Xerox Desert Rose* solar car on day 5 is shown in Fig. 2. The data show the following.

- The SoC was taken from nearly 60 A h at the start of the day to less than 5 A h at the finish. This was based on the expectation of good weather for the charging periods.
- The battery voltage started to fall away at 10 A h. Consequently, the vehicle speed was reduced to conserve energy.
- Strong head winds were encountered late in the afternoon. This accounts for the slower speeds, yet similar power consumption.

5. Li-ion battery configuration

When determining what sort of battery to use, a number of factors must be considered. These include minimization of weight and maximization of both battery efficiency and, of course, cost. This is the reason why lead–acid batteries are still extremely popular with solar car teams who operate on low budgets.

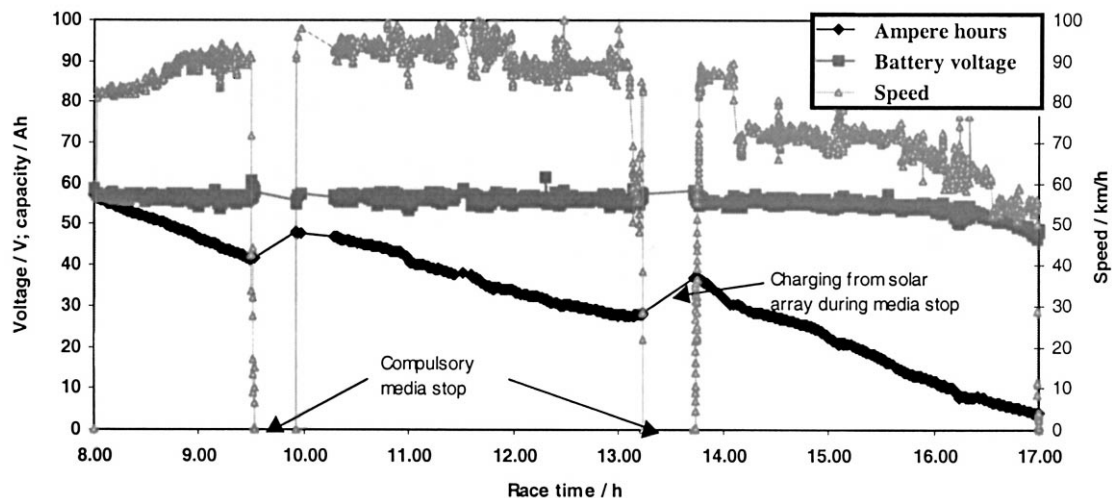


Fig. 2. Telemetry data from *Fuji Xerox Desert Rose* on fifth day of 1999 WSC.

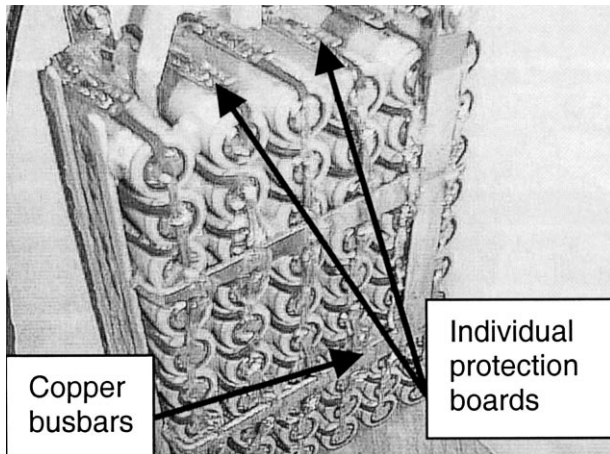


Fig. 3. Li-ion module (60 cells).

The cell chosen by the *Fuji Xerox Desert Rose* team was the NEC ICR18650E Li-ion design made by NEC Moli Energy. The basic specifications of this cell are [2]: voltage, 3.7 V; capacity, 1.7 A h (typical); weight, 43 g (44 g maximum); life, 500 cycles. The cell was selected on the basis of the following criteria.

- High specific energy, viz., 146 W h/kg; in previous events, silver–zinc cells were used with a specific energy of ~ 125 W h/kg.
- Good life; the cells will last the life of the solar car, whereas silver–zinc batteries last only a single race.
- Lower cost; a comparable pack of silver–zinc cells costs an additional US\$10 000.
- Greater reliability and handleability; silver–zinc cells used in previous events proved unreliable when cycled to deep SoCs. Problems encountered included cracking of cells, which resulted in electrolyte leakage.
- Adaptability to existing electronics designed for a 48-V nominal bus; this is easily achievable with Li-ion batteries.

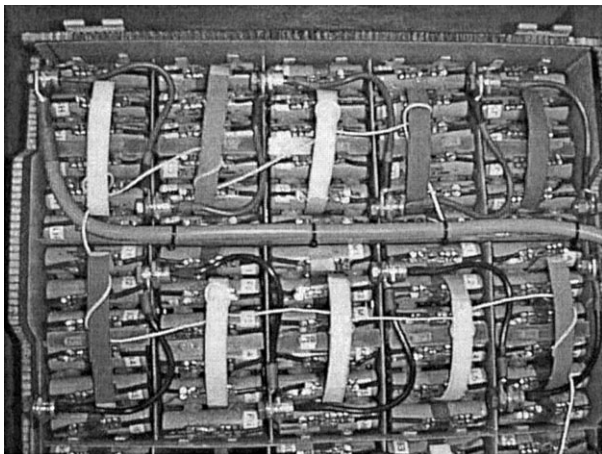


Fig. 4. Ten Li-ion modules viewed from above (bypass diodes shown on top of cells).

The following configuration of cells was therefore devised for the vehicle:

- 60 cells in parallel to form one module (Fig. 3)
- 15 modules in series, i.e., 900 cells in total, to form the battery pack (Fig. 4)
- total battery weight: 39.6 kg, or 47 kg when including busbars, protections and battery box
- bus voltage: 55.5 V; maximum bus: 64.8 V
- total nominal capacity: 102 A h at 55.5 V, i.e., 5.6 kW h

6. Comparison of Li-ion and silver–zinc battery configurations

A comparison of the two different battery types used in the *Fuji Xerox Desert Rose* (silver–zinc in 1996, Li-ion in 1999) is given in Table 1. The data was obtained both from the solar car telemetry and from pre-race testing. The weight includes that of the box and all interconnects.

The coulombic efficiency was calculated by measuring the ampere hours put into the battery and ampere hours taken out of the battery over a full charge–discharge cycle. The ‘Labview’ program was used to monitor Ah-in and Ah-out.

The energy efficiency, the ratio of the joules-out to joules-in over a complete cycle, was calculated in several ways. First, the battery pack was put on charge at 20 A and the voltage was measured. Immediately following a discharge current of 20 A was established, the voltage was remeasured. The ratio of these two voltages gives an indication of the energy efficiency, with further tests post-race required for more accurate results.

Two different tests were conducted post race, which were used to calculate energy efficiency. First, the voltage at a particular SoC was recorded during both charge and discharge. These voltages were recorded and were used to calculate the efficiency. This result, once again, only gave an indication of energy efficiency with further tests still required.

A more accurate way to calculate energy efficiency is to measure the joules-in and joules-out of the battery between a predefined SoC window. This was conducted between 10

Table 1
Comparison of lithium-ion and silver–zinc cells

	Li-ion	Silver–zinc
Bus voltage (average measured) (V)	57	48
Capacity (measured) (A h)	106	126
Capacity (W h)	6042	6048
Coulombic efficiency (%)	100	100
Energy, or charge–discharge, efficiency (%)	95	81
Total weight (kg)	47	40

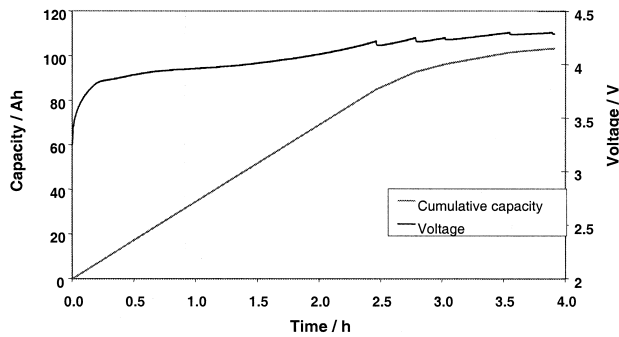


Fig. 5. Capacity and voltage vs. time.

and 80 A h for both charge and discharge and corresponds to the linear charge–discharge region. The curves, shown in Figs. 5 and 6, outline the results used to calculate efficiency via counting the joules-in and joules-out of the battery. All three methods showed the same efficiency, viz., $\sim 95\%$. This value also includes the losses due to the MOSFETs used on the protection boards (see later), which are calculated at 0.7%. Similarly, joules-in and joules-out were computed over a complete cycle of a silver–zinc battery and an efficiency of 81% was calculated. The data were obtained from a previous WSC race.

A comparison of the available energy from the batteries, or the actual energy used to propel the vehicle, can now be made between Li-ion and silver–zinc batteries during race conditions. This is achieved by calculating the total energy from the solar array and multiplying this by the battery efficiency.

Under perfect meteorological conditions, about 2.2 kW h could be stored in the batteries from the solar array of the *Fuji Xerox Desert Rose* during the combined evening and morning charges. If it is assumed that, during racing, all the energy from the sun is used by the vehicle, then the total extra energy available from the morning and afternoon charging periods, as well as before the start of the race, can be calculated.

The available energy at the beginning of the race is given in Table 2, together with the calculated available energy from the morning and afternoon charging periods.

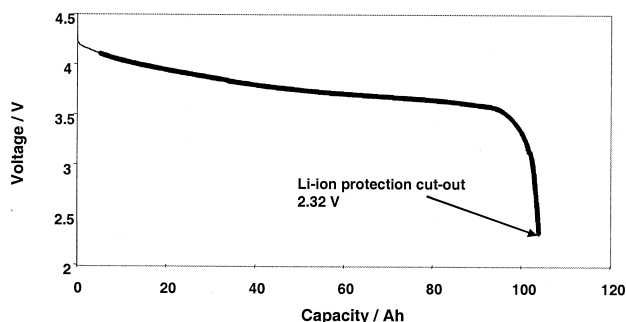


Fig. 6. Li-ion discharge characteristics at 20 A.

Table 2

Total energy available for the race

	Li-ion Silver–zinc	
Initial capacity (measured) (W h)	6042	6048
Morning/afternoon energy available (W h) — 4 days	8800	8800
Energy, or charge–discharge, efficiency (%)	96	81
Actual energy stored in batteries during race (W h)	8448	7128
Total race capacity (W h)	14490	13176

This shows the real advantage of Li-ion battery packs over a silver–zinc counterpart. Even though the Li-ion battery pack weighs slightly more because of the multiplicity of interconnects and protection circuits, the increase in efficiency provides a much greater available energy. This equates to a speed increase of approximately 1 km/h over the whole race for an assumed average speed of 75 km/h.

7. Construction of Li-ion battery pack

The real disadvantage of present Li-ion batteries for use in electric vehicles is their small physical cell size and, hence, small stored capacity. As already mentioned, 900 cells were required for the battery pack of the *Fuji Xerox Desert Rose* solar car.

Commercial units of 10 cells in parallel (= 1 string), which were connected via spot-welded tabbing material with individual protection boards for each cell, were purchased.¹ Six of these strings were then soldered together and joined via nickel-plated, 1-mm thick, copper busbars to make one module. These busbars were tapered according to the magnitude of the current flowing through the copper. Nominally, the *Fuji Xerox Desert Rose* consumes 1 kW of power throughout the day when running at 78 km/h. This corresponds to a nominal current of 18 A from the batteries. Thus, copper busbars and all cabling within the vehicle were sized according to a current density of 1.25 A/mm² or, using the aforementioned current density, a cross-sectional area of 15 mm². This low current density results from a power-to-weight trade-off [3] which, in brief, is a calculation of the power required to carry each kg within the vehicle.

Thermal considerations were also a concern in designing the battery pack. A gap of 1.5 mm was left between each string of 10 cells to allow sufficient air flow, and adequate ventilation holes were provided in the bottom of the battery box. It was subsequently found that, even under the severest load, the batteries did not heat up to any significant extent.

¹ Contact Johnny Grzan at angmo72@hotmail.com

8. Charge–discharge characteristics

Before the race, each 3.7-V battery module was charged separately. A constant-current throughout the linear region followed by constant voltage was found to obtain the greatest stored energy. The linear region is shown in Fig. 5 and is that region where the voltage is approximately linear for a constant-current charge rate.

The method used to charge the batteries is shown in Fig. 7. A $C/3$ rate is used to charge the batteries until 4.2 V/cell is reached. This is followed by progressively decreasing the current in order to keep a relatively constant voltage at a maximum of 4.32 V/cell. This voltage is stabilized overnight to an average of 4.29 V/cell. The lower value is due to the fact that, under charge, the voltage is slightly higher because of the battery’s internal resistance.

The variation of voltage with SoC, using the charging technique shown in Fig. 7, is presented in Fig. 5. The battery module could be charged to a peak SoC of 106 A h, or 1.76 A h/cell.

Of equal importance, particularly to solar car teams, is the discharge performance of the batteries. A constant load of approximately 20 A from the module is shown in Fig. 6. This equates to driving the solar car at just above 78 km/h without sun. Of most importance to solar car teams is the ‘knee’ point of the discharge curve, i.e., the point at which the voltage starts to fall rapidly. The car will still travel after this point, but the speed will be reduced and hill climbing will prove very difficult.

9. Protection of Li-ion batteries

Safety concerns regarding Li-ion batteries have led to the development of specialized integrated circuits (ICs) to protect against damaging the battery and, hence, causing battery failure. Such an IC, fitted with two small MOSFETs, sense resistors, capacitors, fuses, etc. and a small printed-circuit board, was used in the *Fuji Xerox Desert Rose*. A schematic of the protection circuit is presented in Fig. 8 [4]. In normal operation, the MOSFET switches, FET1 and FET2, are both closed. The power consumed by

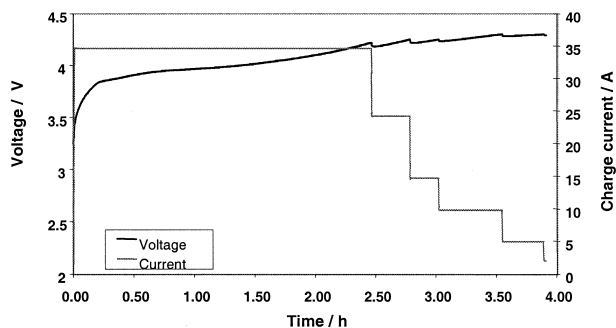


Fig. 7. Charging regime per battery module.

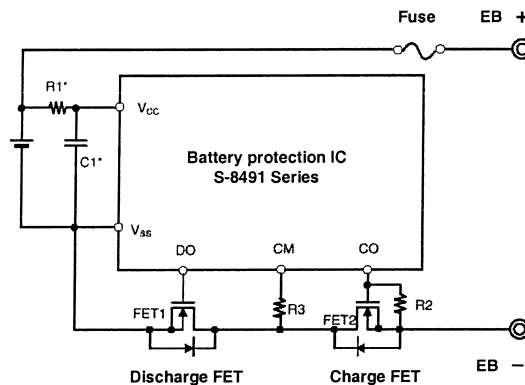


Fig. 8. Schematic of Li-ion protection circuit.

all ICs and all MOSFETs for the complete pack equates to 6.6 W (under 1 kW discharge).

The printed-circuit boards are designed to protect small numbers of cells. Problems arise both in paralleling large numbers of cells and connecting these parallel strings in series to form a high-voltage pack. In particular, this type of protection is not designed to interrupt high currents as the semiconductor switches have a low current rating.

A problem could result when parallel cells are disconnected one-by-one from the module. Under a high load, up to 100 A will be discharged from each module of 60 cells in parallel, i.e., each cell contributes 1.67 A. If a cell is disconnected, the remaining cells have to provide extra current. At a low SoC, this could result in more cells being disconnected so that, eventually, one cell tries to provide all the 100 A. This would result in the destruction of the MOSFET and the associated printed-circuit board.

The protection board offers three different forms of protection namely: (i) overvoltage with a hysteresis band; (ii) undervoltage with a hysteresis band; (iii) an overcurrent trip. The hysteresis band for overvoltage and undervoltage is shown in Fig. 9 [4].

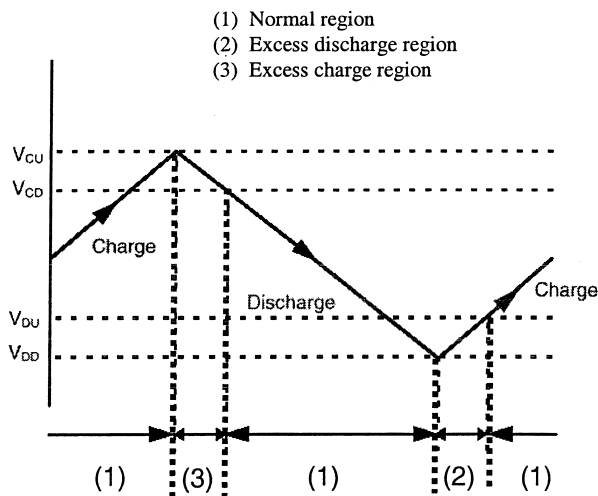


Fig. 9. Mode of operation of protection board.

The hysteresis band is the region between V_{CU} and V_{CD} during charge, and between V_{DD} and V_{DU} during discharge. Considering the charging hysteresis band, the voltage V_{CU} is the maximum voltage to which the cell can be charged before disconnection from the circuit. This cell is only reconnected once V_{CU} minus the hysteresis band, or V_{CD} is reached. A similar analogy applies to the discharge hysteresis band.

Protection mode (i) prevents overcharging of the cell. If the cell voltage exceeds V_{cu} , the charge switch FET2 opens and disables charging to the cell. The switch will close once the voltage falls below V_{cd} . If this mode of protection is activated in a cell and a normal load is applied, the cell will start to discharge when the module bus voltage reaches 3.55 to 3.65 V. This is equal to the cell voltage minus the drop (~ 0.7 V) across the body diode of the charge switch FET2. This load will ultimately bring the cell voltage below V_{cd} and the switch will again close to equalize the cell and bus voltages. The problem this presents is that if, in a pack of 60 cells in parallel, overcharging occurs and the cells turn off, the various protection MOSFETs will turn back on at different times due to production differences. At typical loads, this could result in a small number of the cells providing power until they reach 20% SoC. The remaining cells of the module will then turn back on and produce an inefficient discharge regime.

The following methods were used (both in the laboratory and in the vehicle) to reset the mode of overvoltage shutdown.

- A small resistor (1.5Ω) was connected momentarily across each individual cell. This reduced the cell voltage to below V_{CD} such that the protection board IC reset the charge switch FET2 to on. This cannot be done within the vehicle, as access to each individual cell is not available.
- Within the solar car, resetting can be achieved by putting a large capacitor across the battery pack, i.e., a discharged motor controller capacitor. A discharged capacitor is effectively a short circuit for a brief period of time. Therefore, as charging begins, this capacitor will cause a high inrush current from the battery pack that results in the cell voltage falling below V_{CD} briefly, due to the internal resistance of the cell. This, in turn, results in resetting of the overvoltage mode of each of the protection boards.

The second method is convenient for resetting the overvoltage mode, as it will preferentially shutdown those modules in which not all cells are connected. For a given high current load, in a single module, as one cell trips so the current required from the other cells increases. This results in a ‘domino’ effect, which means that the protection on the last cell of the module will interrupt a very high current. A side effect is that the cell voltage can also drop below V_{DD} . This results in the undervoltage lock-out mode, which can be reset as described below.

Protection mode (ii) prevents excessive discharge from the cell (i.e., low battery voltage). If the cell voltage drops below V_{DD} , the discharge switch FET1 will turn off and

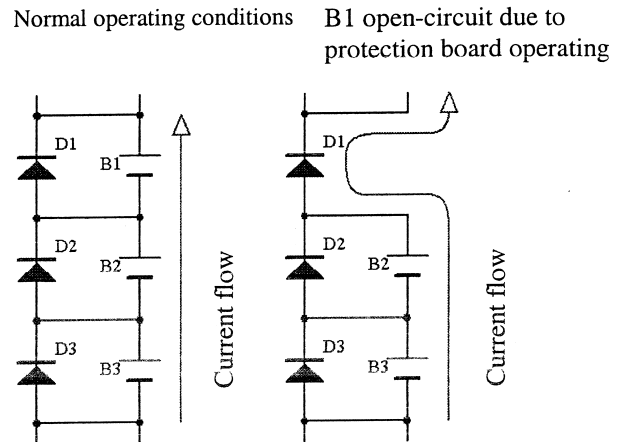


Fig. 10. Schematic of bypass diode.

prevent further discharge. Two conditions must be fulfilled to reset this mode of operation. First, the cell voltage must be above V_{DU} and, second the module bus voltage, connected to a charger (or solar array), must be greater than 2.0 V and supplying a small current.

Protection mode (iii) prevents excessive discharge current (overcurrent) from the cell. Once again, the discharge switch FET1 turns off, but this time it does not latch. To reset, the load resistance must be increased above 50 M Ω . This mode was activated several times within the solar car as a pre-charge circuit for the motor controller did not initially exist. Interestingly, initial tests did not find this to be a problem as the solar array was continually plugged in (i.e., constant reset). This mode was only found during trialing without the solar array.

The Li-ion battery also has an internal seal as an ultimate protection device. The seal will blow if the internal pressure goes too high.

Implemented into the battery pack were bypass diodes, as shown in Fig. 10. These diodes allow current to continue to flow if all of one module's protection boards operate and the complete module goes, open-circuit. Therefore, if one module is on open-circuit, the vehicle can still be driven until time is available to reset the protection mode.

The bypass diodes also protect the ICs of the protection boards. In the case of the protection board shutting down one module, the battery pack effectively reverse biases itself across the protection circuit, i.e., -55 V appears across the IC. Testing this in the laboratory resulted in the destruction of the IC. Thus, implementation of the bypass diodes protects the IC against the module reverse biasing.

10. Testing of protection boards

A procedure was implemented to test every protection board on every cell individually. First under no load, the

voltage of each cell was compared with the module bus voltage. These voltages should be equal, and for those that were found not to be, the protection boards were replaced. Second, a $C/5$ discharge test was performed and the voltage measured. This was to confirm that the charge switch FET2 was on and conduction was not through the body diode of the switch. A 30-mV drop should be seen from the module bus voltage to the cell voltage. A $C/5$ charge test was then implemented to determine that switch FET 1 was turned on and not conducting through its body diode. Lastly, a full discharge (until cut-off) and a full charge (until cut-off) of each module were conducted and the voltage monitored after each cut-off. This series of tests will reveal any faulty protection boards. Between 15 and 20 of the boards were found faulty out of the 900 received. In addition, two suspect Li-ion cells were identified.

11. Conclusions

Li-ion batteries for use in electric vehicles are a very promising technology to provide longer range, a high lifetime, and a very high efficiency. The small size available and safety concerns demand that time and care must be exercised in order to make a reliable and safe battery pack. If this is done, the batteries should perform reliably and pose no safety threat. For solar-car racing, these

batteries will become the batteries of choice for medium-to-large budget teams.

Acknowledgements

The *Fuji Xerox Desert Rose Solar Car Team* would like to thank all their sponsors, namely: Fuji Xerox — The Document Company, Northern Territory University, Holden, Integrated Technical Services, CEANET Technical Computing Solutions, The Math Works, Gulf Transport, Michelin Tyres, Perkins Shipping, N.T. Power and Water Authority and the NTU Sport Association. The authors are also grateful to Dr. D.A.J. Rand for his support and ongoing discussions.

References

- [1] D.M. Roche, A.E.T. Schinckel, J.W.V. Storey, C.P. Humphris, M.R. Guelden, in: *Speed of Light — The 1996 World Solar Challenge*, Photovoltaics Special Research Centre, University of New South Wales, Sydney, Australia, 1997, pp. 7–9.
- [2] NEC Data Sheet — Lithium-Ion Rechargeable Battery — ICR18650E, NEC Moli Energy.
- [3] Patterson, D.J., An efficiency optimized controller for a brushless d.c. machine, and loss measurement using a simple calorimetric technique, Record of the 26th Annual IEEE Power Electronics Specialist Conference, PESC'95, Atlanta, pp. 22–27.
- [4] Seiko Battery Protection IC Data Sheet — S-8491 Series, Seiko Instruments.